Simplified model of the convex obstacles transition zone diffraction for carrier UWB signal propagation

Piotr Górniak*, Wojciech Bandurski+

#Poznań University of Technology, Department of Electronics and Telecommunication
Polanka 3, Poznań, Poland
pgorniak@.et.put.poznan.pl

+ Poznań University of Technology, Department of Electronics and Telecommunication
Polanka 3, Poznań, Poland
wojciech.bandurski@..put.poznan.pl

Abstract— **The paper presents the derivation of a 2D time-domain model of two bare perfectly conducting convex obstacles for the case of UWB carrier signal propagation. The model includes amplitude diffraction and first order transition zone diffraction, called the slope diffraction. The considered model is represented by its impulse response. Thanks to the introduction of some vital approximations of the expressions occurring in amplitude term and slope term of the impulse response, it can be given in a closed form. The presented approach is extended for the case of more than two cascaded convex obstacles in the channel. The Uniform Theory of Diffraction (UTD) formulated in the frequency domain is used in the derivation of the model. The correctness and accuracy of the derived model is verified by simulation of an Ultra Wide Band (UWB) midband pulse distortion.**

I. Introduction

The paper presents the time domain (TD) modelling of diffraction caused by convex objects. We consider the soft polarization case. We propose to use deterministic UWB channel modelling for the channel with convex objects. Examples of such objects are round buildings, round pillars in buildings and rounded corridors in buildings. In our considerations, the transition zone diffraction is included. Therefore the slope diffraction is the key factor and cannot be omitted. When the UWB signal propagation is taken into account, the time domain modelling is the right choice.

In the paper we present the closed form formula for the impulse response of two cascaded, perfectly conducting convex obstacles shadowing the transmitter and the receiver. We base on the impulse response – h(t) of two convex obstacles derived in [1]. When h(t) is applied to a calculation of a response of the convex obstacles for an incident UWB signal, the complexity of a particular simulation of an UWB pulse propagation may be too high for more complex scenarios. When bigger amount of convex obstacles occur in a signal path, the complexity of calculations grows fast. The h(t) from [1] has also a shortcoming, which will be outlined in this paper. To overcome these problem we present in this paper the improvement of the impulse response derived in [1]. We transform the impulse response given in [1] into a lot more profitable form for UWB EM wave propagation tools. For the purpose of doing it we introduce some vital approximations whose application enables to simplify the impulse response. After obtaining the new formula for two convex obstacles impulse response we describe the way of derivation of the impulse responses of more than two convex obstacles.

In Section 2 of the paper there is shown the geometrical model of two convex obstacles for the case of transition zone diffraction, as well as the impulse response of the model described in [1]. Section 3 gives the method of transforming h(t) into a lot less complex form and extension of the method to more than two convex obstacles case. The simulations results are presented in Section 4. Section 5 gives the conclusions.

II. The Model of Two Convex Obstacles for Transition Zone Case

The model of two cascaded convex obstacles is shown in Fig. 1. The parameters of the convex obstacles are described in [3]. When two convex obstacles are taken into account, and the second obstacle is in the transition zone of the first convex obstacle, the frequency response of the "partial" channel has the following form [1]:

$$[H_s(\omega, s) + H_A(\omega)]A(s)e^{-jk(\theta_1 R_{H1}+s)}, \qquad (2.1)$$

where s is equal to distance $|Q_1Q_2'|$, A(s) is the spreading factor, the input of the channel is at point Q_1' and the output

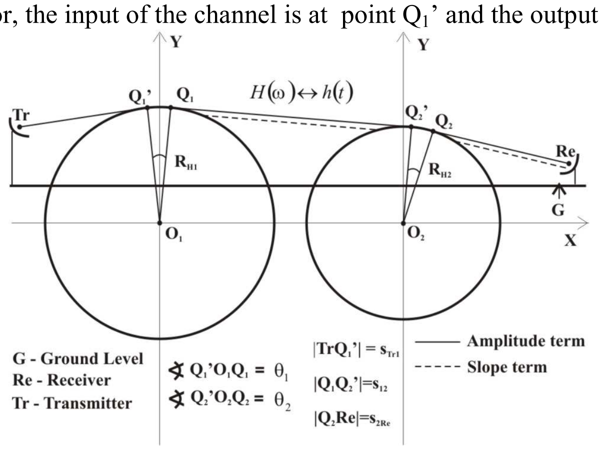

Fig. 1 Two cascaded convex obstacles shadowing the transmitter and receiver.

of the channel is at point Q_2 (Fig. 1). The slope term and amplitude term of (2.1) are related through the following equation:

$$H_s(\omega,s)=\frac{\partial H_A(\theta)}{s\partial\theta} \tag{2.2}$$

The formulas for $H_A(\omega)$ and $H_S(\omega,s)$ are given in [1]. In the model we assume that the slope of the field is zero when the field originates from the transmitter. We further assume that the receiver is in the far zone, so the slope of the field originating from the second obstacle equals zero. Then the TD field at the receiver is defined by (2.3) [1,2] (time delay of the signal over the distance $\theta_{1/2}R_{1/2}$ is not included):

$$E_{\mathrm{Re}}(t)=\left(E_2(t)*h_A(t,L_{A12\mathrm{Re}},R_2,\theta_2)+\frac{\partial E_2(t)}{\partial n}*d(t,L_{s12\mathrm{Re}},R_2,\theta_2)\right)\ldots \tag{2.3}$$
$$A_2(s)*\delta\left(t-\frac{s_{2\mathrm{Re}}}{c}\right),$$

where:

$$E_2(t)=E_1(t)*h_A(t,L_{ATr12},R_1,\theta_1)*\delta\left(t-\frac{s_{12}}{c}\right)A_1(s),$$

$$\frac{\partial E_2(t)}{\partial n}=E_1(t)*h_s(t,L_{sTe12},R_1,\theta_1,s_{12})*\delta\left(t-\frac{s_{12}}{c}\right)A_1(s),$$

E_1 is the function of the field at point Q_1', where the creeping ray hits the first convex object, L_{A12Re} and L_{S12Re} are the distance parameters ensuring the continuity of the amplitude term and slope term of the field around the shadow boundary after the second convex object [2], and L_{ATr12} and L_{STr12} are the distance parameters ensuring the continuity of the amplitude term and slope term of the field around the shadow boundary after the first convex object [2].

When the spreading factor and delay terms are omitted the impulse response of the two convex obstacles is given by:

$$h(t)=h_A(t,L_{ATr12},R_1,\theta_1)*h_A(t,L_{A12\mathrm{Re}},R_2,\theta_2)+\ldots \tag{2.4}$$
$$h_s(t,L_{sTe12},R_1,\theta_1,s_{12})*d(t,L_{s12\mathrm{Re}},R_2,\theta_2).$$

For midband UWB propagation the formulations for the factors occurring in (2.4) have the following forms:

$$h_A(t,N)=A(L,R,\theta)\cdot\frac{1}{\sqrt{t(t+a(L,\theta))}}+\ldots \tag{2.5}$$
$$\sum_{n=0}^{N}Aq_n(R,\theta)\mathrm{Re}\left\{j^{-\frac{1}{6}}I_A(t,\alpha(R,\theta))\right\},$$

$$h_S(t,s,N)=S_1(L,R,\theta,s)\cdot\frac{\partial}{\partial t}\left(\frac{1}{\sqrt{t(t+a(L,\theta))}}\right)+S_2(L,R,\theta,s)\cdot\frac{1}{\left(\sqrt{t}\right)^3}+\ldots \tag{2.6}$$
$$S_3(R,\theta,s)\cdot\frac{1}{\sqrt{t}}+\sum_{n=0}^{N}Sq_n(R,\theta,s)\mathrm{Re}\left\{j^{\frac{1}{6}}I_S(t,\alpha(R,\theta))\right\},$$

$$d(t,s,N)=D_1(L,R,\theta,s)\cdot\frac{1}{\sqrt{t(t+a(L,\theta))}}+D_2(L,R,\theta,s)\cdot\frac{1}{\left(\sqrt{t}\right)}+\ldots \tag{2.7}$$
$$D_3(R,\theta,s)\cdot\sqrt{t}+\sum_{n=0}^{N}Dq_n(R,\theta,s)\cdot\mathrm{Re}\left\{j^{-\frac{5}{6}}I_D(t,\alpha(R,\theta))\right\},$$

where $A(L,R,\theta)$, $Aq_n(L,R,\theta)$, $S_{1/2}(L,R,\theta,s)$, $Sq_n(L,R,\theta,s)$, $D_{1/2}(L,R,\theta,s)$, $Dq_n(L,R,\theta,s)$, are the constants dependent on the convex obstacles parameters and the scenario. Functions $I_A[\omega,t,\alpha(R,\theta)]$, $I_s[\omega,t,\alpha(R,\theta)]$. $I_D[\omega,t,\alpha(R,\theta)]$, are presented in (2.8a-c).

$$I_A[t,\alpha(R,\theta)]=\frac{1}{\pi}\int_0^\infty\omega^{-\frac{1}{6}}e^{-\alpha(R,\theta)(j\omega)^{\frac{1}{3}}}e^{j\omega t}d\omega \tag{2.8a}$$

$$I_S[t,\alpha(R,\theta)]=\frac{1}{\pi}\int_0^\infty\omega^{\frac{1}{6}}e^{-\alpha(R,\theta)(j\omega)^{\frac{1}{3}}}e^{j\omega t}d\omega \tag{2.8b}$$

$$I_D[t,\alpha(R,\theta)]=\frac{1}{\pi}\int_0^\infty\omega^{-\frac{5}{6}}e^{-\alpha(R,\theta)(j\omega)^{\frac{1}{3}}}e^{j\omega t}d\omega \tag{2.8c}$$

The "early time" solutions of (2.8a-c) my be obtained by performing expansion of the exp(jωt) factor around $\omega t=0$ and the "late time" solutions by using expansion exp[-$\alpha(R,\theta)\cdot(j\omega)^{1/3}$] around $\omega^{1/3}=0$. Then by applying the definition of the gamma function the approximate solutions of 2.8a-c for the case of "early time" and "late time" may be given by Eq. 2.9a-c and 2.10a-c respectively.

$$I_A(t,\alpha(R,\theta))\approx\frac{3}{(\alpha(R,\theta))^{\frac{5}{2}}\pi}\sum_{m=0}^{M}\frac{(j)^m}{m!}\left(\frac{-jt}{(\alpha(R,\theta))^3}\right)^m\Gamma\left[3\left(m+\frac{5}{6}\right)\right] \tag{2.9a}$$

$$I_S(t,\alpha(R,\theta))\approx\frac{3}{(\alpha(R,\theta))^{\frac{7}{2}}\pi}\sum_{m=0}^{M}\frac{(j)^m}{m!}\left(\frac{-jt}{(\alpha(R,\theta))^3}\right)^m\Gamma\left[3\left(m+\frac{7}{6}\right)\right] \tag{2.9b}$$

$$I_D(t,\alpha(R,\theta))\approx\frac{3}{(\alpha(R,\theta))^{\frac{1}{2}}\pi}\sum_{m=0}^{M}\frac{(j)^m}{m!}\left(\frac{-jt}{(\alpha(R,\theta))^3}\right)^m\Gamma\left[3\left(m-\frac{1}{6}\right)\right] \tag{2.9c}$$

$$I_A(t,\alpha(R,\theta))\approx\frac{1}{(-jt)^{\frac{5}{6}}\pi}\sum_{m=0}^{M}\frac{j^{-\frac{m}{3}}}{m!}\left(\frac{(\alpha(R,\theta))^3}{-jt}\right)^{\frac{m}{3}}\Gamma\left[\frac{m}{3}+\frac{5}{6}\right] \tag{2.10a}$$

$$I_S(t,\alpha(R,\theta))\approx\frac{1}{(-jt)^{\frac{7}{6}}\pi}\sum_{m=0}^{M}\frac{j^{-\frac{m}{3}}}{m!}\left(\frac{(\alpha(R,\theta))^3}{-jt}\right)^{\frac{m}{3}}\Gamma\left[\frac{m}{3}+\frac{7}{6}\right] \tag{2.10b}$$

$$I_D(t,\alpha(R,\theta))\approx\frac{1}{(-jt)^{\frac{1}{6}}\pi}\sum_{m=0}^{M}\frac{j^{-\frac{m}{3}}}{m!}\left(\frac{(\alpha(R,\theta))^3}{-jt}\right)^{\frac{m}{3}}\Gamma\left[\frac{m}{3}+\frac{1}{6}\right] \tag{2.10c}$$

In order to find any shortcoming of the above approximations, "early time" and "late time" expressions were examined through the series of numerical calculations. After examination it turned out that both series are convergent for limited range of argument $TH=t/\alpha(R,\theta)^3$. The series from (2.10) are convergent for bigger values of TH and the series from (2.9) are convergent for smaller values of TH. With the usage of (2.10) the real part of the expressions given by:

$$u_A(t,R,\theta)=j^{-\frac{1}{6}}I_A(t,\alpha(R,\theta)) \tag{2.11a}$$

$$u_S(t,R,\theta)=j^{\frac{1}{6}}I_S(t,\alpha(R,\theta)) \tag{2.11b}$$

$$u_D(t,R,\theta)=j^{-\frac{5}{6}}I_D(t,\alpha(R,\theta)) \tag{2.11c}$$

can be approximated very well for bigger values of TH. The values of minimum TH for given M and the maximum relative error of (2.11) approximation set to 0,2% are presented in Table I.

TABLE I
MINIMUM VALUE OF TH FOR A GIVEN M AND THE ERROR OF APPROXIMATION OF (2.11) SET TO 0,2%.

M	TH_{min}	M	TH_{min}	M	TH_{min}
5	0,99994	17	0,02362	35	0,00429
6	0,38992	18	0,01789	36	0,00375
7	0,35016	19	0,01864	37	0,00387
8	0,19573	26	0,00845	38	0,00358
9	0,10751	27	0,00705	39	0,00316
10	0,10862	28	0,00731	40	0,00325
11	0,07588	29	0,00657	41	0,00302
12	0,04915	30	0,00558	42	0,00269
13	0,05043	31	0,00577	43	0,00277
14	0,03854	32	0,00525	44	0,00259
15	0,02785	33	0,00453	45	0,00233
16	0,02896	34	0,00468	46	0,00239

Opposite quality of approximation of (2.11) occurs when (2.9) is applied. With the usage of the series (2.9) there can be only approximated only imaginary part (2.11). The real part of (2.11) is 0. The same conclusion was obtained in [5]. This signifies that the first series cannot be used for approximation of (2.5-2.7) for smaller values of TH. Even for values of TH for which the series from (2.9) is convergent the real part of (2.11) is about 10^3. The reason of this approximation error is the way of solving integrals (2.8) for early time. The factor exp(jωt) were expanded about ωt=0, what is equivalent of expanding of functions sin(ωt) and cos(ωt) around ωt=0. For bigger values of ωt (the upper limit of the integrals in (2.8) is infinity) the expansion used are not valid and the result of the integrals, with exp(jωt) and with expanded exp(jωt), differs much. In order to solve this problem we propose another way of approximation of (2.11). We took advantage over the fact that the real parts of (2.11) can be approximated for bigger values of TH by the functions:

$$ur_{A>}(t,R,\theta) \approx t^{-\frac{5}{6}} \cdot R_A(TH) \tag{2.12a}$$

$$ur_{S>}(t,R,\theta) \approx t^{-\frac{7}{6}} \cdot R_S(TH) \tag{2.12b}$$

$$ur_{D>}(t,R,\theta) \approx t^{-\frac{1}{6}} \cdot R_D(TH) \tag{2.12c}$$

where R_A(TH), R_S(TH), R_D(TH) are the functions dependent only on the value of TH.

We stated the thesis that for all values of TH the approximation of the real parts of (2.11) must be of similar form:

$$ur_A(t,R,\theta) \approx t^{-\frac{5}{6}} \cdot Y_A(TH) \tag{2.13a}$$

$$ur_S(t,R,\theta) \approx t^{-\frac{7}{6}} \cdot Y_S(TH) \tag{2.13b}$$

$$ur_D(t,R,\theta) \approx t^{-\frac{1}{6}} \cdot Y_D(TH) \tag{2.13c}$$

where the functions Y_A(TH), Y_S(TH), Y_D(TH) coincide with the functions R_A(TH), R_S(TH), R_D(TH) respectively for bigger values of TH. Our statement that the real parts of (2.11) must be approximated by the function formed by multiplication of $t^{-5/6}$ or $t^{-7/6}$ or $t^{-1/6}$ with the function dependent only on the TH argument were, examined numerically. We analyzed if the functions:

$$X_A(t,\alpha) = ur_A(t,R,\theta) \cdot t^{\frac{5}{6}} \tag{2.14a}$$

$$X_S(t,\alpha) = ur_S(t,R,\theta) \cdot t^{\frac{7}{6}} \tag{2.14b}$$

$$X_D(t,\alpha) = ur_A(t,R,\theta) \cdot t^{\frac{1}{6}} \tag{2.14c}$$

are dependent only on the value of TH argument. After examination of (2.14) for the wide scope of t and $\alpha(R,\theta)$ values we proved the thesis.

Then we approximated (2.14). From available approximation functions we chose the following series:

$$X_A(t,\alpha) \approx \sum_{n=1}^{7} a_{An} \cdot t^{\frac{12+n}{6}} \tag{2.15a}$$

$$X_S(t,\alpha) \approx \sum_{n=1}^{7} a_{Sn} \cdot t^{\frac{14+n}{6}} \tag{2.15b}$$

$$X_S(t,\alpha) \approx \sum_{n=1}^{7} a_{Dn} \cdot t^{\frac{8+n}{6}} \tag{2.15c}$$

where a_{A1}-a_{A7}, a_{S1}-a_{S7}, a_{D1}-a_{D7}, are the constants which can be found through the process of optimization of the approximation error. With the usage of our optimization algorithm we found the constants and we obtained the approximations results shown in Fig. 2.

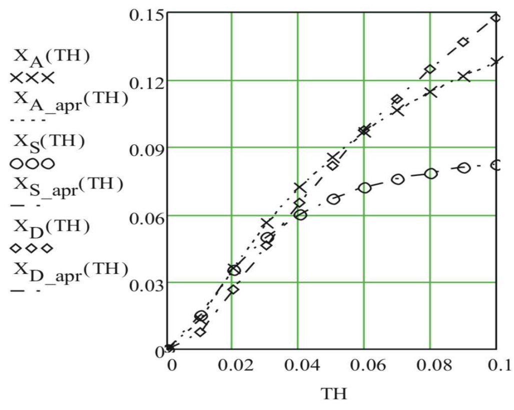

Fig. 2. Functions (2.14) and its approximating series - (2.15)

In Fig. 2 X_{A_apr}(TH), X_{S_apr}(TH), X_{D_apr}(TH), are the approximations of X_A(TH), X_S(TH), X_D(TH) respectively. After applying (2.15), the real parts of (2.11) can be approximated by the series (for t=0 (2.14) is 0) :

$$u_{rA}(t,\alpha) \approx \sum_{n=1}^{7} a_{An} \cdot t^{\frac{7+n}{6}} \tag{2.16a}$$

$$u_{rS}(t,\alpha) \approx \sum_{n=1}^{7} a_{Sn} \cdot t^{\frac{7+n}{6}} \tag{2.16b}$$

$$u_{rD}(t,\alpha) \approx \sum_{n=1}^{7} a_{Dn} \cdot t^{\frac{7+n}{6}} \tag{2.16c}$$

Now almost all of the components in (2.5-2.7) are the rational powers of t (besides the first in (2.5-2.7)).

III. Simplifications of the Convex Obstacles Impulse Response

The main contribution to complexity of the calculation of response of two convex obstacles for an UWB pulse give the numerical operations of convolutions occurring in (2.4). In order to solve this problem we calculate these convolutions. A problem arises during calculation of the convolutions of functions containing singularities. If we need to calculate convolutions $x_1(t)*x_2(t)$ and at least one of the functions contain singularity at t=0, we proceed as follows. To remove singularities**,** we integrate $x_1(t)$ n times (if necessary), and we integrate $x_2(t)$ m times (if necessary). As a result we obtain:

$$\underbrace{\int \ldots \int}_{n} x_1(t)dt * \underbrace{\int \ldots \int}_{m} x_2(t)dt = y_1{}^{n}(t) * y_2{}^{m}(t) = p(t) \tag{3.1}$$

Next we differentiate p(t) m+n times to obtain:

$$x_1(t) * x_2(t) = \frac{\partial^{n+m}}{t^{n+m}} p(t) \tag{3.2}$$

The procedure is applied to each convolution appearing in expression (2.4), after substitution (2.15) to (2.5-2.7) and further (2.5-2.7) to (2.4). Most of the functions $y_1{}^n(t)$ and/or $y_2{}^m(t)$ are proportional to $t^{(7+n)/6}$ (n=1,2..7), $t^{1/2}$ and t, in other words time cores - ***TCs*** - of most $y_1{}^n(t)$ and/or $y_2{}^m(t)$ are $t^{(7+n)/6}$ and $t^{1/2}$. Unfortunately, functions $y_1{}^n(t)$ and/or $y_2{}^m(t)$ in some cases have TCs equal to $\mathrm{arctg}[(B_i t)^{1/2}]$, where B_i is the constant calculated for i-th convex obstacle in the specific scenario. Then convolution (3.1) cannot be obtained in the analytical way. In that case function $\mathrm{arctg}[(B_i t)^{1/2}]$ is approximated by the following expression:

$$C_a(t) = \begin{cases} a_1{}^k B_i t + a_0{}^k \sqrt{B_i t} & for \quad B_i t < (B_i t)_T \\ a_3{}^k + \dfrac{a_2{}^k}{\sqrt{B_i t}} & for \quad B_i t \geq (B_i t)_T \end{cases}, \tag{3.3}$$

where k=1 or 2.

Parameters $a_n{}^k$ (n=0, 1, 2, 3) and the threshold argument $(B_i t)_T$ are determined by a optimization algorithm (e.g. genetic algorithm).

After applying approximation (3.3) all $y_1{}^n(t)$ and $y_2{}^m(t)$ functions are constituted by the components which can be convoluted analytically. For early time - $B_i t<(B_i t)_T$ – the results of the convolutions of the TCs which have to be calculated in order to derive two convex obstacles impulse response are given in Table II.

Table II
Results of the convolutions of TCs of $y_1{}^n(t)$ and $y_2{}^m(t)$ – q(t) for $B_i t<(B_i t)_T$ for 2 convex obstacles

Convoluted TCs	q(t)
$\sqrt{t} * \sqrt{t}$	$\frac{\pi}{8} \cdot t^2$
$\sqrt{t} * t^{\frac{7+n}{6}}$	$\frac{5+2n}{3(16+n)} \frac{\Gamma\left(\frac{3}{2}\right)\Gamma\left(\frac{5}{2}\right)}{\Gamma\left(\frac{16+n}{6}\right)} \cdot t^{\frac{17+n}{6}}$
$t^{\frac{7+m}{6}} * t^{\frac{7+n}{6}}$	$\frac{6}{n+13} {}_2F_1\left(\frac{-(m+7)}{6}, \frac{n+13}{6}, \frac{n+19}{6}, 1\right) \cdot t^{\frac{21+n+2m}{6}}$
$t * t^u$	$\frac{1}{(u+1)(u+2)} \cdot t^{2+u} \quad u \in \left\{\frac{7+n}{6}, \frac{1}{2}, 1\right\}$

Functions $\Gamma(x)$ and ${}_2F_1(a_1,a_2,b_1,1)$ are the gamma function and the generalized hypergeometric function respectively [4].

Using the results from Table II we can give the formulation for the simplified impulse response of two convex obstacles:

$$h_2(t) = h_{2A}(t) + h_{2S}(t) \tag{3.4}$$

where:

$$h_{2A}(t) = A_{22} \cdot t + A_{21} \cdot \sqrt{t} + A_{20} + \sum_{n=1}^{7} Aq_{2n} \cdot t^{\frac{11+n}{6}} + \sum_{n=1}^{7} Ap_{2n} t^{\frac{13+n}{n}} + \sum_{n=1}^{7}\sum_{m=1}^{7} Ar_{2nm} \cdot t^{\frac{21+n+2m}{6}} \tag{3.5}$$

$$h_{2S}(t) = S_{21} + \frac{S_{20}}{\sqrt{t}} + \sum_{n=1}^{7} Sq_{2n} \cdot \left(t^{\frac{11+n}{6}} + t^{\frac{5+n}{6}}\right) + \sum_{n=1}^{7} Sp_{2n} \left(t^{\frac{13+n}{6}} + t^{\frac{7+n}{6}}\right) + \sum_{n=1}^{7}\sum_{m=1}^{7} Sr_{2nm} \cdot t^{\frac{21+n+2m}{6}} \tag{3.6}$$

where A_{22}, A_{21}, A_{20}, Aq_{2n}, Ap_{2n}, $Ar_{2nm,}$ S_{21}, S_{20}, Sq_{2n}, Sp_{2n}, Sr_{2nm} are the functions of the parameters of the convex obstacles and the appropriate constants from Table II.

Having the form of the impulse response of two convex obstacles, we can extend the presented method for more than 2 convex obstacles in cascade. By analysing (3.5) and (3.6) and knowing the "convolutions form" impulse response of 3 convex obstacles in cascade given by:

$$\begin{aligned} h_3(t) &= \left(h_{2A}(t) + h_{2S}(t)\right) * \left(h_S^2 t) * d^3(t) + h_A^3(t)\right) = \\ &= h_2(t) * h_S^2 t) * d^3(t) + h_2(t) * h_A^3(t) \end{aligned} \tag{3.7}$$

where Superscript 2 or 3 in $h_S{}^2(t)$, $d^3(t)$ $h_A{}^3(t)$ means that the functions depend on the parameters related to 2nd or 3rd obstacle, we can give TCs of $y_1{}^n(t)$ and $y_2{}^m(t)$ which have to be convoluted for the case of 3 obstacles in cascade. These are $t^{(7+n)/6}$ (n=1,2..7), $t^{(7+k)/6}$ (k=-1,0,1..15,19,20..33,35), $t^{1/2}$,t and t^0. For early time - $B_i t<(B_i t)_T$ – the results of the convolutions of the TCs which have to be calculated in order to obtain the impulse response of 3 convex obstacles in cascade are given in Table III.

Table III
Results of the convolutions of TCs of $y_1^n(t)$ and $y_2^m(t)$ – q(t) for $B_i t<(B_i t)_T$ for 3 convex obstacles

Convoluted TCs	q(t)
$\sqrt{t}*\sqrt{t}$	$\frac{\pi}{8}\cdot t^2$
$\sqrt{t}*t^{\frac{7+n}{6}}$	$\frac{5+2n}{3(16+n)}\frac{\Gamma\left(\frac{3}{2}\right)\Gamma\left(\frac{5}{2}\right)}{\Gamma\left(\frac{16+n}{6}\right)}\cdot t^{\frac{17+n}{6}}$
$\sqrt{t}*t^{\frac{7+k}{6}}$	$\frac{5+2k}{3(16+k)}\frac{\Gamma\left(\frac{3}{2}\right)\Gamma\left(\frac{5}{2}\right)}{\Gamma\left(\frac{16+k}{6}\right)}\cdot t^{\frac{17+k}{6}}$
$t^{\frac{7+k}{6}}*t^{\frac{7+n}{6}}$	$\frac{6}{k+13}\,{}_2F_1\left(\frac{-(n+7)}{6},\frac{k+13}{6},\frac{k+19}{6},1\right)\cdot t^{\frac{21+k+2n}{6}}$
$t*t^u$	$\frac{1}{(u+1)(u+2)}\cdot t^{2+u}\quad u\in\left\{\frac{7+n}{6},\frac{7+k}{6},\frac{1}{2},1\right\}$
t^0*t^u	$\frac{1}{u+1}\cdot t^{u+1}\quad u\in\left\{\frac{7+n}{6},\frac{7+k}{6},\frac{1}{2},1,0\right\}$

By analysing Table III we can give the simplified form of the impulse response for 3 convex obstacles in cascade:

$$h_3(t)=h_{3A}(t)+h_{3S}(t) \tag{3.8}$$

where:

$$h_{2A}(t)=\sum_{m=0}^{3}A_{3m}\cdot t^{\frac{m}{2}}+\sum_{m=1}^{15}Aq_{3m}\cdot t^{\frac{11+m}{6}}+ \sum_k\left(A1p_{3k}t^{\frac{11+k}{6}}+A2p_{3k}t^{\frac{13+k}{6}}\right)+\sum_k\sum_{n=1}^{7}Ar_{3kn}t^{\frac{21+k+2n}{6}} \tag{3.9}$$

$$h_{2A}(t)=\sum_{m=0}^{4}S_{3m}\cdot t^{\frac{m}{2}}+\sum_k\sum_{n=1}^{7}Sr_{3kn}t^{\frac{21+k+2n}{6}} \sum_k\left(S1p_{3k}t^{\frac{11+k}{6}}+S2p_{3k}t^{\frac{13+k}{6}}+S3p_{3k}t^{\frac{17+k}{6}}+S4p_{3k}t^{\frac{19+k}{6}}\right) \tag{3.10}$$

where A_{3m}, Aq_{3m}, $A1p_{3k}$, $A2p_{3k}$, Ar_{3kn}, S_{3m}, Sq_{3m}, $S1p_{3k}$, $S2p_{3k}$, $S3p_{3k}$, $S4p_{3k}$ Sr_{3kn} are the functions of the parameters of the convex obstacles and the appropriate constants from Table II and Table III:

IV. Verification of the simplified impulse response.

The correctness of the derived simplified impulse response is verified in the process of simulation of the distortion of a particular midband UWB pulse, given by (4.1). We made the numerical calculations in MathCad environment. We compared the results, obtained using the simplified impulse response, with the IFFT (applied to the UTD frequency response of the convex obstacles) results, Fig. 3.

$$tp(t)=\left(\frac{8\cdot k}{\pi}\right)^{\frac{1}{4}}\frac{1}{\sqrt{1+e^{\frac{2\pi^2 f_c^2}{k}}}}e^{-k\cdot t^2}\cos(2\pi f_c\cdot t) \tag{4.1}$$

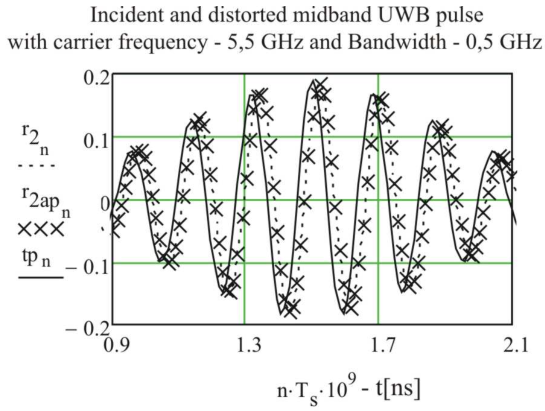

Fig. 3. The shape the incident and distorted UWB pulse caused by diffraction on two convex obstacles in cascade (t_c=1.5 ns).

In Fig. 3. the results (samples) of the pulse distortion obtained with IFFT (r_{2n}) are compared with the results of the pulse distortion obtained through simplified direct time domain calculations (r_{2apn}) and with incident UWB pulse normalized to the amplitude of the distorted pulse (tp_n). The values of parameters of the convex objects are θ_1=0.02 rad, θ_2=0.018 rad, R_1=0.4m and R_2=0.25m (Fig. 1).

V. Conclusions

In the paper we present the procedure for obtaining the simplified time domain formulas for the impulse response of 2 cascaded convex obstacles in the case of carrier UWB signal propagation. The extension of the procedure for the case of more than 2 convex obstacles in cascade is also shown. Numerical experiments show that the results obtained using the approximations presented in Section 3 are accurate when compared to the results obtained by IFFT. However the former were obtained at a lot smaller complexity cost and therefore it is a lot more profitable to use it in simulation tools. Although (2.4) relates to the soft polarization case, respective formulas can be derived for hard polarization, using a similar method to that applied for the soft polarization case. Further research should concern the non-good conducting convex obstacles scenario.

References

[1] P. Górniak, W. Bandurski “Direct Time Domain Analysis of an UWB Pulse Distortion by Convex Objects With the Slope Diffraction Included” IEEE Transactions on Antennas and Propagation., vol. 56, September 2008, pp. 3036–3044.

[2] G. Koutitas, C. Tzaras, “A UTD Solution for Multiple Rounded Surfaces”, IEEE Transactions on Antennas and Propagation, vol. 54, no. 4, April 2006, pp 1277-1283.

[3] H. L. Bertoni, “Radio propagation for modern wireless systems”, Upper Saddle River, N. Jersey, 2000.

[4] M. Abramowitz, I. A. Stegun, “Handbook of Mathematical Functions”.

[5] P. R. Rousseau, P. H. Pathak, Hsi-Tseng Chou, “A time domain formulation of the uniform geometrical theory of diffraction for scattering from a smooth convex surface”, IEEE Transactions on Antennas and Propagation, vol. 55, no. 6, June 2007, pp. 1522-1534